Hindawi
Advances in Condensed Matter Physics
Volume 2017, Article ID 5652763, 7 pages
https://doi.org/10.1155/2017/5652763

Research Article

External Electric Field Effect on Shallow Donor Impurity States in Zinc-Blende $In_xGa_{1-x}N$/GaN Symmetric Coupled Quantum Dots

Guang-Xin Wang,[1] Li-Li Zhang,[2] and Huan Wei[1]

[1]*College of Science, North China University of Science and Technology, Tangshan 063000, China*
[2]*Publishing Management Center, North China University of Science and Technology, Tangshan 063000, China*

Correspondence should be addressed to Guang-Xin Wang; guangxinwang@126.com

Received 18 July 2017; Accepted 12 September 2017; Published 28 November 2017

Academic Editor: Gongxun Bai

Copyright © 2017 Guang-Xin Wang et al. This is an open access article distributed under the Creative Commons Attribution License, which permits unrestricted use, distribution, and reproduction in any medium, provided the original work is properly cited.

Based on the effective-mass approximation and variational procedure, the ground-state donor binding energy in a cylindrical zinc-blende $In_xGa_{1-x}N$/GaN symmetric coupled quantum dots (SCQDs) is investigated in the presence of the external electric field. Numerical results show that the donor binding energy increases firstly until a maximum value, and then it begins to drop quickly in all the cases with decreasing the dot radius. As the thickness of left dot and right dot decreases, the donor binding energy increases monotonically at first, reaches a maximum value, and then drops rapidly for an impurity ion located at the right dot center and the middle barrier center. Moreover, the donor binding energy for an impurity ion located at the center of the left dot is insensitive to the variation of dot thickness for large dot thickness due to the Stark effect. Meanwhile, the impurity position plays an important role on the change of the donor binding energy under the external electric field. In particular, the impurity position corresponding to the peak value of the donor binding energy is shifted toward the left QD with increasing the external electric field strength.

1. Introduction

Recent advances in modern fabrication techniques have made it possible to grow wide-band-gap GaN-based low-dimensional semiconductor quantum structures [1, 2] and $In_xGa_{1-x}N$ ternary alloys, as one of the most important members of the group III nitride semiconductor family such as quantum wells (QWs), quantum well wires (QWWs), and quantum dots (QDs), and have attached considerable attention due to their unique electronic and optical properties, as well as their potential applications in electronics and optoelectronic devices [3, 4]. Using molecular-beam epitaxy and metal-organic chemical-vapor deposition methods, the distance between two material layers can precisely be controlled within a few angstroms experimentally. Therefore, the coupling effects between adjacent dots become significant and cannot be neglected, and their electronic structure and optical properties may be adjusted effectively. In the past many years, much theoretical and experimental work have been devoted in investigating electronic structure and binding energy of a hydrogenic impurity in different shape QDs [5–19]. Liu et al. [5] studied the oscillator strengths of the optical transitions of vertically stacked self-assembled InAs quantum disks. Dong et al. [6] studied single-electron and two-electron vertically assembled quantum disks in an axial magnetic field using the effective-mass approximation. Liu et al. [7] theoretically analyzed the influence of compressive stress on shallow donor impurity states in symmetric GaAs/Al_xGa_{1-x}As double quantum dots. L. Z. Liu and J. J. Liu studied [8] hydrogenic-donor impurity states in coupled quantum disks in the presence of a magnetic field. Wang [9] also investigated the ground-state donor binding energy and the average interparticle distances for a hydrogenic impurity in double quantum dots by using variational method. Pressure-dependent shallow donor binding energies have been reported in single QDs [10] and coupled QDs [11]. Xia et al. [12] investigated hydrostatic pressure effect of donor impurity states in zinc-blende (ZB) InGaN/GaN asymmetric

coupled quantum dots. Several factors affect the binding energy of an impurity ion, including the applied external perturbation (magnetic field, hydrostatic pressure), the size of QDs, the barrier thickness, and the position of the donor ion.

On the other hand, applying an external electric field is also a powerful tool to change the electronic and optical properties of low-dimensional semiconductor structures. The Stark effect of donor impurity states in a QD is a major subject for QD physics and applications [13, 14]. The external electric field effect on donor binding energy has been the subject of intensive investigation [15–19]. Xia et al. studied the hydrogenic impurity states in ZB InGaN single QD in the absence of the applied electric field (GaN/AlN coupled QDs) [15, 16]. Jiang et al. [17, 18] presented the external electric field influence on the donor binding energy in a ZB GaN/AlGaN cylindrical (spherical) QD. We also investigated the combined effects of an intense laser field, electric field, and hydrostatic pressure on donor impurity states in zinc-blende InGaN/GaN quantum dots [19].

However, as we know, multiple QDs rather than single QD are adopted in the commonly used GaN-based optoelectronic devices. And few papers are involved in investigating the shallow donor impurity states in ZB $In_xGa_{1-x}N$/GaN SCQDs under the external electric field to date. Thus, it is necessary to study the external electric field effect of the donor impurity states in ZB GaN-based coupled QDs. In this paper, using effective-mass approximation and variational procedure, we report the calculation of ground-state donor binding energy in coupled QDs in the presence of an electric field along the growth direction of the SCQDs. The effects of the structure parameters of the SCQDs, the impurity position, and the applied electric field are all taken into account. This work is organized as follows: in Section 2 we present our theoretical framework, the numerical results are discussed in Section 3, and finally, the conclusions are given in Section 4.

2. Theoretical Framework

2.1. Hamiltonian. Within the effective-mass approximation, the Hamiltonian for a hydrogenic impurity in a cylindrical ZB $In_xGa_{1-x}N$/GaN SCQDs under the influence of applied electric field F in the z-direction, as shown in Figure 1, may be written by [8]

$$\widehat{H} = \widehat{H_0} - \frac{e^2}{4\pi\varepsilon_0\varepsilon\left|\vec{r} - \vec{r}_0\right|} \tag{1}$$

with

$$\widehat{H_0} = -\frac{\hbar^2}{2m^*_{w,b}}\left[\frac{1}{\rho}\frac{\partial}{\partial\rho}\left(\rho\frac{\partial}{\partial\rho}\right) + \frac{1}{\rho^2}\frac{\partial^2}{\partial\varphi^2} + \frac{\partial^2}{\partial z^2}\right] - \frac{e^2}{\varepsilon_{w,b}\left|\vec{r} - \vec{r}_0\right|} + V(\rho, z) + e\vec{F}z, \tag{2}$$

where $|\vec{r} - \vec{r}_0| = [\rho^2 + (z - z_0)^2]^{1/2}$ is the distance between an impurity ion and the electron. F is the applied electric field along the SCQDs growth direction. The subscripts w and b stand for dot layer and barrier layer materials, respectively. $m^*_{w,b}$ and $\varepsilon_{w,b}$ are the conduction effective masses and dielectric constants of dot layer and barrier layer, respectively. $V(\rho, z)$ is the radial and z-direction confinement potential due to the conduction band offset in ZB $In_xGa_{1-x}N$/GaN SCQDs, which can be given as follows [10]:

$$V(\rho, z) = \begin{cases} V(\rho) & \rho \le R,\ \rho > R \\ V(z) & z < -\dfrac{L_{\mathrm{mb}}}{2},\ -\dfrac{L_{\mathrm{mb}}}{2} \le z \le \dfrac{L_{\mathrm{mb}}}{2},\ z > \dfrac{L_{\mathrm{mb}}}{2} \end{cases}$$

$$V(\rho) = \begin{cases} 0 & \rho \le R \\ V_0 & \rho > R \end{cases}$$

$$V(z) = \begin{cases} V_0 & z < -\dfrac{(L_{\mathrm{lw}} + L_{\mathrm{mb}})}{2} \\ 0 & -\dfrac{(L_{\mathrm{lw}} + L_{\mathrm{mb}})}{2} < z < -\dfrac{L_{\mathrm{mb}}}{2} \\ V_0 & -\dfrac{L_{\mathrm{mb}}}{2} \le z \le \dfrac{L_{\mathrm{mb}}}{2} \\ 0 & \dfrac{L_{\mathrm{mb}}}{2} < z < \dfrac{(L_{\mathrm{rw}} + L_{\mathrm{mb}})}{2} \\ V_0 & z > \dfrac{(L_{\mathrm{rw}} + L_{\mathrm{mb}})}{2}, \end{cases} \tag{3}$$

where $V_0 = Q[E_g(\mathrm{GaN}) - E_g(In_xGa_{1-x}N)]$. $E_g(\mathrm{GaN})$ and $E_g(In_xGa_{1-x}N)$ are the band gap energies of the materials GaN and $In_xGa_{1-x}N$, respectively. In order to calculate the ground-state donor binding energy in ZB $In_xGa_{1-x}N$/GaN SCQDs, the trial wave function may be written as follows [11, 12]:

$$\phi(\rho, \phi, z) = Nf(\rho)h(z)e^{il\phi}e^{-\lambda\rho^2 - \beta(z - z_0)^2}, \quad l = 0, \pm1, \pm2, \ldots, \tag{4}$$

where N is the normalization constant and λ and β are variational parameters. Former $f(\rho)$ and latter $h(z)$ are the radial and the axial wave functions, respectively. The former can be obtained through the Bessel function J_m and the modified Bessel function K_m, while the latter can be expressed by means of the Airy functions Ai and Bi. l is the electron z-component angular momentum quantum number. The former is given by [19]

$$f(\rho) = \begin{cases} J_0(\alpha\rho) & \rho \le R \\ \dfrac{J_0(\alpha R)}{K_0(\tau R)}K_0(\tau\rho) & \rho > R, \end{cases} \tag{5}$$

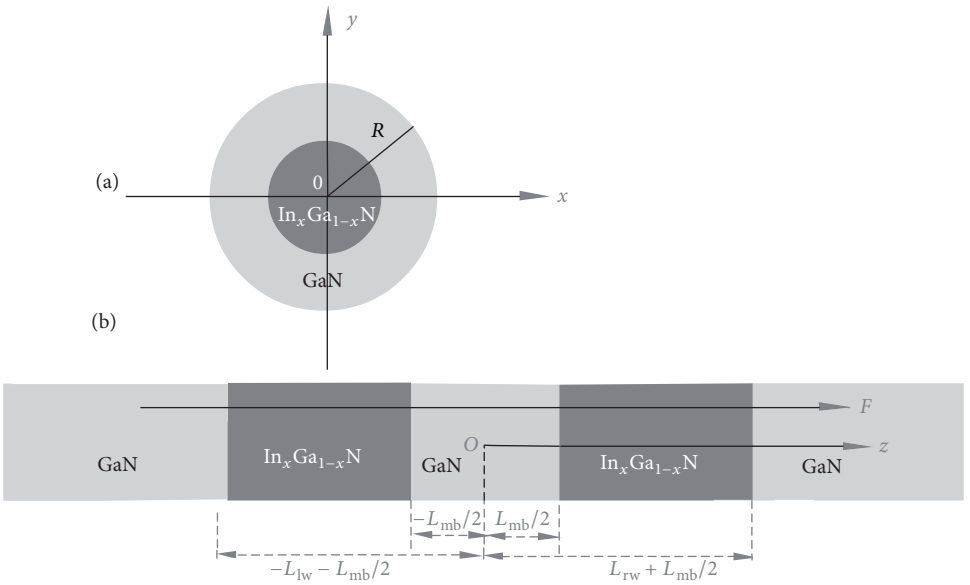

FIGURE 1: A diagram of a cylindrical ZB $In_xGa_{1-x}N$/GaN symmetric coupled QDs of the radius R, the left dot height L_{lw}, the middle barrier width L_{mb}, and the right dot height L_{rw}. The z-axis is defined to be the growth direction of the SCQDs, and the external electric field is applied along z-axis of the coupled QDs.

where the constants (α and τ) in (5) are determined from the continuity of the derivative of the radial wave function at the SCQDs boundary. The latter is given by

$$h(z) = \begin{cases} C_1 \mathrm{Ai}(\varepsilon_1) + D_1 \mathrm{Bi}(\varepsilon_1) & -L_b - L_{lw} - \dfrac{L_{mb}}{2} < z \le -L_{lw} - \dfrac{L_{mb}}{2} \\ C_2 \mathrm{Ai}(\varepsilon_2) + D_2 \mathrm{Bi}(\varepsilon_2) & -L_{lw} - \dfrac{L_{mb}}{2} < z \le -\dfrac{L_{mb}}{2} \\ C_3 \mathrm{Ai}(\varepsilon_3) + D_3 \mathrm{Bi}(\varepsilon_3) & -\dfrac{L_{mb}}{2} < z \le \dfrac{L_{mb}}{2} \\ C_4 \mathrm{Ai}(\varepsilon_4) + D_4 \mathrm{Bi}(\varepsilon_4) & \dfrac{L_{mb}}{2} < z \le L_{rw} + \dfrac{L_{mb}}{2} \\ C_5 \mathrm{Ai}(\varepsilon_5) + D_5 \mathrm{Bi}(\varepsilon_5) & L_{rw} + \dfrac{L_{mb}}{2} < z < L_{rw} + \dfrac{L_{mb}}{2} + L_b. \end{cases} \quad (6)$$

Here $\varepsilon_j = ((2m^*_{w,b}(p)/\hbar^2)eF)^{1/3}(z - E_z - V(z)/eF)$. The coefficients C_j and D_j ($j = 1, 2, 3, 4$, and 5) of the eigenfunction $h(z)$ at the interfaces can be obtained by using transfer matrix methods [20]. The ground-state donor impurity energy is evaluated by minimizing the expectation value of the Hamiltonian with respect to the parameters λ and β. With the adiabatic approximation, the donor binding energy of a hydrogenic impunity E_b is defined as the difference between the ground-state energy of the system with and without impurity; that is, [20]

$$E_b = E_{0\rho} + E_{0z} - \min_{\lambda,\beta} \frac{\langle \psi \mid H \mid \psi \rangle}{\langle \psi \mid \psi \rangle}, \quad (7)$$

where $E_{0\rho}$ and E_{0z} are the radial and the axial ground-state energies of the electron in ZB $In_xGa_{1-x}N$/GaN SCQDs, respectively.

3. Results and Discussion

We have calculated the ground-state donor binding energy E_b as functions of the dot radius R, the dot thickness L ($L_{lw} = L_{rw} = L$), the middle barrier width L_{mb}, the impurity positions z_0, and the applied electric field F in a ZB $In_xGa_{1-x}N$/GaN SCQDs. All parameters used in the present paper are the same as in [21]. The electron effective mass is $m^*_w = [0.2(1-x)+0.12x]m_0$ for $In_xGa_{1-x}N$ material and $m^*_b = 0.2m_0$ for GaN material [21], and m_0 is the free space electron mass. The band gap energy of ZB $In_xGa_{1-x}N$ of indium composition x can be given as follows [21]: $E_g(In_xGa_{1-x}N) = 0.78x + 3.52(1 - x) - 1.4x(1 - x)$. The band offset ratio is assumed to be 80 : 20. The concentration x in the $In_xGa_{1-x}N$ material is selected as 0.15.

The ground-state donor binding energy in a ZB $In_xGa_{1-x}N$/GaN SCQDs is displayed in Figure 2 as a function of the dot radius for different external electric fields ($F = 0$, 30, and 50 kV/cm). The impurity ion is located at the left dot center ($z_0 = -(L_{lw} + L_{mb})/2$). It can be seen obviously in Figure 2 that the donor binding energy increases firstly until a maximum value, and then it begins to drop quickly in all the cases with the decrease of the dot radius. The behavior is related to the variation of the electron confinement in ZB $In_xGa_{1-x}N$/GaN SCQDs. The electron wave function is more firmly localized inside the QD with decreasing the dot radius, and the Coulomb interaction between the electron and the impurity ion is enhanced, so the donor binding energy increases correspondingly. However, below a certain value of the radius, the donor binding energy starts decreasing due to leakage of the electron wave function into the barrier region. In addition, curves (1–3) also display that the donor binding energy becomes larger with the increase of the applied electric field. This can be explained that as

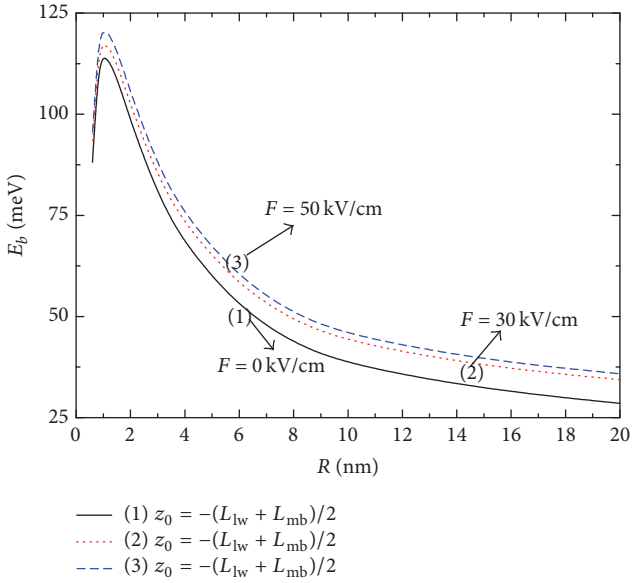

FIGURE 2: The ground-state donor binding energy E_b in a ZB $In_xGa_{1-x}N$/GaN symmetric coupled QDs as a function of the dot radius R with L_{lw} = 5 nm, L_{mb} = 1 nm, L_{rw} = 5 nm, ρ_0 = 0. In these calculations were considered three values of the applied electric field—zero (curve 1), F = 30 kV/cm (curve 2), and F = 50 kV/cm (curve 3).

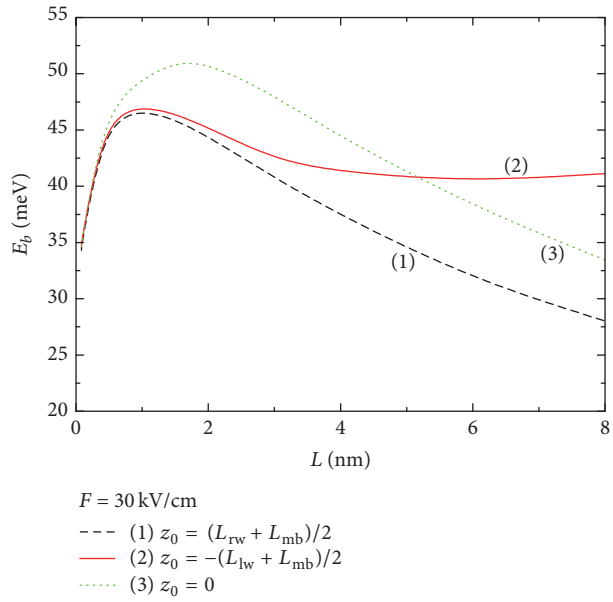

FIGURE 3: The ground-state donor binding energy E_b in a ZB $In_xGa_{1-x}N$/GaN symmetric coupled QDs as a function of the QD thickness L (L_{lw} = L_{rw} = L) for R = 10 nm, L_{mb} = 1 nm, F = 30 kV/cm, ρ_0 = 0. Curves 1, 2, and 3 are for the impurity positions $z_0 = (L_{rw} + L_{mb})/2$, $-(L_{lw} + L_{mb})/2$, 0, respectively.

the applied electric field becomes large, the electron wave function can be shifted toward the left QD in the same spatial confinement, thus leading to a larger donor binding energy.

Figure 3 displays the QD thickness effect on the ground-state donor binding energy with the parameters (L_{mb} = 1.0 nm, R = 10 nm, and ρ_0 = 0) for three different positions of the impurity ion: at the right dot center (curve 1), at the left dot center (curve 2), and at the middle barrier center (curve 3). The external electric field along the growth direction of the SCQDs is selected as F = 30 kV/cm. The thickness of left dot and right dot are selected as the same L in the calculation. It can be seen from curves (1 and 3) that the donor binding energy increases monotonically at first, reaches a maximum value, and then drops rapidly as the dot thickness decreases. The physical reason can be explained as follows: the size quantization confinement of the electron wave function goes stronger with decreasing the thickness of left dot and right dot, and the Coulomb interaction between the electron and the impurity ion becomes larger, and the donor binding energy increases correspondingly. When the thickness of left dot and right dot decreases to a certain value, the probability of the electron leaking into barrier region increases greatly, and hence the Coulomb action between the electron and the impurity ion diminishes accordingly. Comparing curve 2 with the others, it is found that the donor binding energy is insensitive (sensitive) to the variation of the dot thickness for large (small) dot thickness for an impurity ion located at the left dot center. This can be explained by the fact that the electron wave function is strongly shifted into the left QD for large dot thickness under the external electric field and has less freedom to penetrate into the right QD. The average distance between the electron and the impurity ion remains almost constant. Moreover, the spatial confinement effect of the electron wave function is much higher than the external electric field effect for smaller dot thickness. When the dot thickness decreases to a certain value, the probability of the electron penetrating into the potential barrier increases greatly, and the Coulomb interaction between the electron and the impurity ion is weakened accordingly. These behaviors can be explained as the competition effects between external electric field and spatial confinement in a ZB $In_xGa_{1-x}N$/GaN SCQDs.

The effect of the middle barrier width on the donor binding energy for different impurity positions with the parameters (R = 10 nm, L_{lw} = 4 nm, L_{mb} = 1 nm, L_{rw} = 4 nm, F = 30 kV/cm) is displayed in Figure 4. It can be seen in Figure 4 that when the middle barrier width L_{mb} is zero, the donor binding energy for the impurity ion located at the center of left dot (curve 1) and right dot (curve 3) is smaller than the one for the impurity ion located at the center of middle barrier (curve 2). These behaviors can be explained as follows. When the middle barrier width goes to zero, the donor binding energy goes to the exact values for a single QD with R = 10 nm and L_w = 8 nm. Therefore, the electron can occupy a larger free space without the middle barrier. The electron cloud is distributed mainly around the impurity position z_0 = 0. The average distance between the electron and the impurity ion decreases, which leads to the increase of the donor binding energy. Curves (1 and 3) demonstrate that the donor binding energy decreases firstly, reaches a minimum value, and then increases gradually as the middle barrier thickness L_{mb} increases. This is because

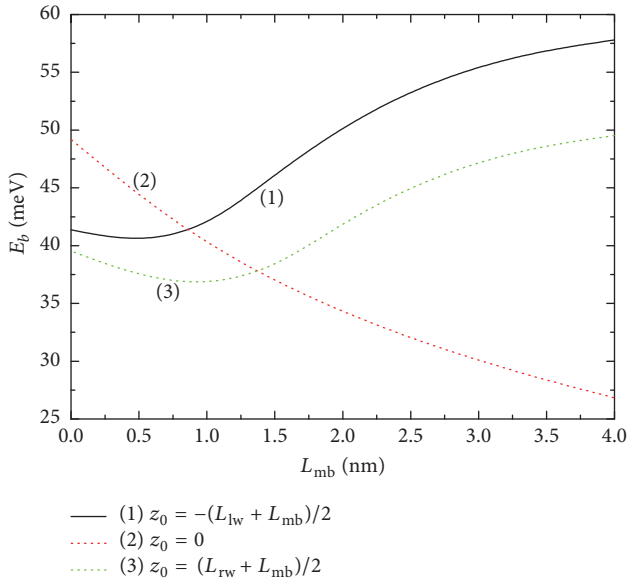

FIGURE 4: The ground-state donor binding energy E_b in a ZB $In_xGa_{1-x}N/GaN$ symmetric coupled QDs as a function of the middle barrier width L_{mb} for $R = 10$ nm, $L_{lw} = 4$ nm, $L_{rw} = 4$ nm, $F = 30$ kV/cm, $\rho_0 = 0$ for different impurity positions z_0.

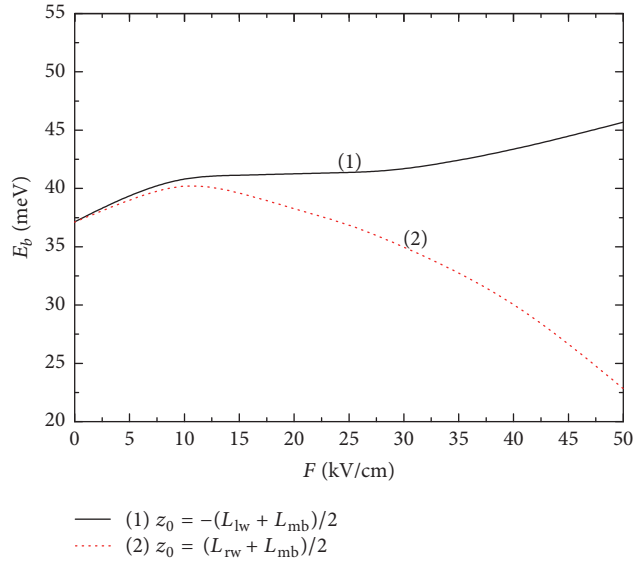

FIGURE 5: The ground-state donor binding energy E_b in a ZB $In_xGa_{1-x}N/GaN$ symmetric coupled QDs as a function of the electric field F for $R = 10$ nm, $L_{lw} = 4$ nm, $L_{mb} = 1$ nm, $L_{rw} = 4$ nm, $\rho_0 = 0$. Curves 1, 2 are for the impurity positions $z_0 = -(L_{lw}+L_{mb})/2$, $(L_{rw} + L_{mb})/2$, respectively.

the two QDs are decoupled due to the existence of the small middle barrier width, and the probability of the electron wave function in left dot and right dot penetrating into the middle barrier becomes larger, which leads to the weakening of the Coulomb interaction between the electron and the impurity ion. Therefore, the donor binding energy decreases slightly. Moreover, when the middle barrier thickness increases to a certain value, the coupling effect between the two QDs on the donor binding energy becomes weaker gradually under the external electric field. The bigger the middle barrier width is, the stronger the localization effect of the electron wave function in left dot and right dot is due to the Stark effect. The probability of the electron wave function confined around the impurity ion becomes large. Therefore, the donor binding energy for the impurity ion located at the center of left dot and right dot increases correspondingly. Comparing curve 1 and curve 2, in the same spatial confinement, the donor binding energy for the impurity ion located at the center of left dot is much larger than the one for the impurity ion located at the center of right dot. This is because that the applied electric field pushes greatly the electron wave function into the left QD of the SCQDs. In addition, curve 2 also demonstrates that the donor binding energy for the impurity ion located at the center of the middle barrier decreases gradually with the increase of the middle barrier width. This is because that the probability of the electron wave function penetrating into the middle barrier becomes small under the external electric field with the increase of the middle barrier width. The Coulomb interaction between the electron and the impurity ion weakens gradually, and the donor binding energy decreases correspondingly.

In Figure 5, the external electric field effect on the ground-state donor binding energy for different impurity positions ($z_0 = -(L_{lw} + L_{mb})/2$ (curve 1), $z_0 = (L_{rw} + L_{mb})/2$ (curve 2)) is showed with the parameters ($R = 10$ nm, $L_{lw} = 4$ nm, $L_{mb} = 1$ nm, $L_{rw} = 4$ nm). For the impurity ion located at the center of the left QD (curve 1), the increase of the applied electric field F leads to an enhancement of the donor binding energy. It is because that as the applied electric field increases, the probability of the electron penetrating into the left dot increases greatly, and the electron is strongly confined around the impurity ion. In addition, curve 2 also shows that the donor binding energy increases firstly, reaches a maximum value, and then decreases gradually. The main reason is as follows: the smaller external electric field enhances the localization effect of the electron wave function in the right dot. The distance between the electron and the impurity ion decreases, which causes the increase of the donor binding energy. When the applied electric field increases to a certain value, the probability of the electron in the right dot leaking into barrier layer and left dot increases greatly, which leads to the decrease of the donor binding energy. In addition, the stronger the applied electric field is, the more significant the change of the donor binding energy is. The same effect has also been observed for vertical-stacked InGaN/GaN multiple-quantum wells [20].

In Figure 6, the ground-state donor binding energy is investigated as a function of the axial position z_0 of the impurity ion in the ZB $In_xGa_{1-x}N/GaN$ SCQDs with the parameters $R = 10$ nm, $L_{lw} = 4$ nm, $L_{mb} = 1$ nm, $L_{rw} = 4$ nm, $\rho_0 = 0$ and with different external electric fields ($F = 0$, 30 kV/cm, and 50 kV/cm). Curve 1 demonstrates that, in the absence of the electric field, the donor binding energy has two maximum values, which are located at the center of left and right QDs and symmetrical with respect to the middle barrier center. This can be understood such that the electric

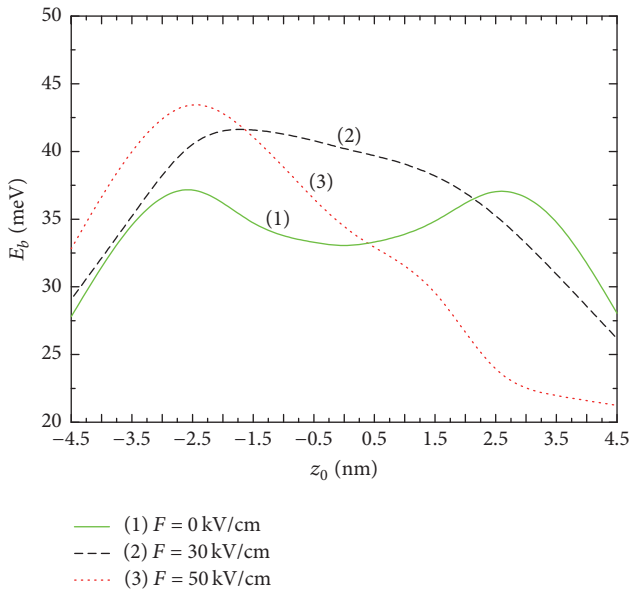

FIGURE 6: The ground-state donor binding energy E_b in a ZB $In_xGa_{1-x}N$/GaN symmetric coupled QDs as a function of the impurity position z_0 for R = 10 nm, L_{lw} = 4 nm, L_{mb} = 1 nm, L_{rw} = 4 nm, ρ_0 = 0 for different external electric field F = 0, 30 kV/cm, and 50 kV/cm.

field effect on the system disappears and leads to the coupled QDs becoming a symmetrical configuration. The electron wave function is strongly and symmetrically confined inside left dot and right dot of the ZB $In_xGa_{1-x}N$/GaN SCQDs in the spatial confinement, and therefore the increment of the Coulomb interaction between the electron and the impurity ion that causes the increase of the donor binding energy. In addition, it may also be seen in curves (2-3) that when the external electric field is applied, only a maximum value is remained. And the impurity position corresponding to the peak value of the donor binding energy is shifted toward left dot of the ZB $In_xGa_{1-x}N$/GaN SCQDs with increasing the external electric field. This is because the applied electric field pushes greatly the electron wave function into left dot of the SCQDs. Figure 6 also demonstrates that the stronger the applied electric field is, the bigger the peak value of the donor binding energy is. It is because the maximum localization effect of the electron wave function in the ZB $In_xGa_{1-x}N$/GaN SCQDs strengthens as the applied electric field increases. As a general feature, these behaviors can be explained as the combined effects between external electric field, quantum confinement, and coupled action of the SCQDs.

4. Conclusion

In conclusion, we have investigated the combined effects of an external electric field, spatial confinement, and coupled action on a shallow donor impurity confined in a cylindrical ZB $In_xGa_{1-x}N$/GaN symmetric coupled QDs. The calculations were performed by using a variational procedure based on the effective-mass approximation. The donor binding energy is investigated as a function of the dot radius, the dot thickness, the external electric field, and the impurity position. Number results can be summarized as follows: (1) as the QD radius increases, the donor binding energy increases firstly until a maximum value, and then it begins to drop quickly in all the cases; (2) as the dot thickness L decreases, the donor binding energy increases monotonically at first, reaches a maximum value, and then drops rapidly for the impurity located at right dot center and middle barrier center. Moreover, the donor binding energy is insensitive to the variation of dot thickness for large dot thickness when the impurity ion is located at the left dot center. (3) When the impurity ion is located at the center of left dot and right dot, respectively, as the middle barrier thickness L_{mb} increases, the donor binding energy decreases firstly, reaches a minimum value, and then increases gradually. And the donor binding energy for the impurity ion located at the center of middle barrier decreases gradually with the increase of the middle barrier width. (4) The external electric field significantly affects the distribution of the electron wave function in the ZB $In_xGa_{1-x}N$/GaN SCQDs. And the electron wave function is shifted toward the left QD under the external electric field. (5) In the absence of the electric field, the donor binding energy has two maximum values, which are symmetrically located on the center of left dot and right dot of ZB $In_xGa_{1-x}N$/GaN SCQDs. When the external electric field is applied, only a maximum value is remained, and the stronger the applied electric field is, the bigger the peak value of the donor binding energy is. The main results obtained in this paper might be suitable for other ZB semiconductor quantum structures. We hope that these calculation results can stimulate further investigations of the physics and device applications of group III nitride materials.

Conflicts of Interest

The authors declare that there are no conflicts of interest regarding the publication of this paper.

Acknowledgments

This work was supported by The Education Department Foundation of Hebei Province (no. QN2015050).

References

[1] A. Lotsari, G. P. Dimitrakopulos, T. Kehagias, A. Das, E. Monroy, and P. Komninou, "Structural properties of semipolar InGaN/GaN quantum dot superlattices grown by plasma-assisted MBE," *Microelectronic Engineering*, vol. 90, pp. 108–111, 2012.

[2] S. Nakamura and S. F. Chichibu, *Introduction to Nitride Semiconductor Blue Lasers and Light Emitting Diodes*, Taylor & Francis, London, UK, 2000.

[3] W. S. Tan, V. Bousquet, M. Kauer, K. Takahashi, and J. Heffernan, "Ingan-based blue-violet laser diodes using AlN as the electrical insulator," *Japanese Journal of Applied Physics*, vol. 48, no. 7, Article ID 072102, 2009.

[4] M. Gladysiewicz, R. Kudrawiec, J. Misiewicz et al., "The surface boundary conditions in GaN/AlGaN/GaN transistor heterostructures," *Applied Physics Letters*, vol. 98, no. 1, Article ID 231902, 2011.

[5] J. L. Liu, S. S. Li, Z. C. Niu, F. H. Yang, and S. L. Feng, "Optical spectra and exciton state in vertically stacked self-assembled quantum discs," *Chinese Physics Letters*, vol. 20, no. 7, pp. 1120–1123, 2003.

[6] Q. R. Dong, S. S. Li, Z. C. Niu, S. L. Feng, and H. Z. Zheng, "Electronic structure of self-assembled InAs quantum disks in an axial magnetic field and two-electron quantum-disk qubit," *Journal of Applied Physics*, vol. 96, no. 6, pp. 3277–3281, 2004.

[7] J. J. Liu, M. Shen, and S. W. Wang, "The influence of compressive stress on shallow-donor impurity states in symmetric GaAs-Ga1-xAlxAs double quantum dots," *Journal of Applied Physics*, vol. 101, no. 7, Article ID 073703, 2007.

[8] L. Z. Liu and J. J. Liu, "Hydrogenic-donor impurity states in coupled quantum disks in the presence of a magnetic field," *Journal of Applied Physics*, vol. 102, no. 3, Article ID 033709, 2007.

[9] X. F. Wang, "Hydrogenic impurity in double quantum dots," *Physics Letters A*, vol. 364, no. 1, pp. 66–69, 2007.

[10] G. X. Wang, X. Z. Duan, and W. Chen, "Barrier thickness and hydrostatic pressure effects on hydrogenic impurity states in wurtzite GaN/$Al_xGa_{1-x}N$ strained quantum dots," *Journal of Nanomaterials*, vol. 2015, Article ID 937310, 9 pages, 2015.

[11] M. Zhang and J. J. Shi, "Influence of pressure on exciton states and interband optical transitions in wurtzite InGaN/GaN coupled quantum dot nanowire heterostructures with polarization and dielectric mismatch," *Journal of Applied Physics*, vol. 111, Article ID 113516, 11 pages, 2012.

[12] C. X. Xia, Z. P. Zeng, Q. Chang, and S. Y. Wei, "Donor impurity states in zinc-blende InGaN/GaN asymmetric coupled quantum dots: Hydrostatic pressure effect," *Physica E: Low-dimensional Systems and Nanostructures*, vol. 42, no. 8, pp. 2041–2046, 2010.

[13] H. El Ghazi, A. Jorio, and I. Zorkani, "Theoretical investigation of stark effect on shallow donor binding energy in InGaN spherical QD-QW," *Physica B: Condensed Matter*, vol. 422, pp. 47–50, 2013.

[14] B. E. Kane, "A silicon-based nuclear spin quantum computer," *Nature*, vol. 393, no. 6681, pp. 133–137, 1998.

[15] C. X. Xia, Y. M. Liu, and S. Y. Wei, "Hydrogenic impurity states in zinc-blende GaN/AlN coupled quantum dots," *Physics Letters A*, vol. 372, no. 42, pp. 6420–6423, 2008.

[16] F. C. Jiang, C. X. Xia, and S. Y. Wei, "Hydrogenic impurity states in zinc-blende InGaN quantum dot," *Physica B: Condensed Matter*, vol. 403, no. 1, pp. 165–169, 2008.

[17] L. M. Jiang, H. L. Wang, H. T. Wu, Q. Gong, and S. L. Feng, "External electric field effect on the hydrogenic donor impurity in zinc-blende GaN/AlGaN cylindrical quantum dot," *Journal of Applied Physics*, vol. 105, no. 5, Article ID 053710, 2009.

[18] L. M. Jiang, H. L. Wang, H. T. Wu, Q. Gong, and S. L. Feng, "External electric field effect on hydrogenic donor impurity in zinc-blende InGaN quantum dot," *Chinese Physics Letters*, vol. 25, no. 8, pp. 3017–3020, 2008.

[19] G. X. Wang, R. Zhou, and X. Z. Duan, "Combined effects of an intense laser field, electric field and hydrostatic pressure on donor impurity states in zinc-blende InGaN/GaN quantum dots," *Journal of the Korean Physical Society*, vol. 69, no. 2, pp. 189–196, 2016.

[20] C. X. Xia, Z. P. Zeng, S. Y. Wei, and J. B. Wei, "Shallow-donor impurity in vertical-stacked InGaN/GaN multiple-quantum wells: electric field effect," *Physica E: Low-dimensional Systems and Nanostructures*, vol. 43, no. 1, pp. 458–461, 2010.

[21] T. Vurgaftman and J. R. Meyer, "Band parameters for III–V compound semiconductors and their alloys," *Journal of Applied Physics*, vol. 94, no. 6, pp. 3676–3696, 2003.

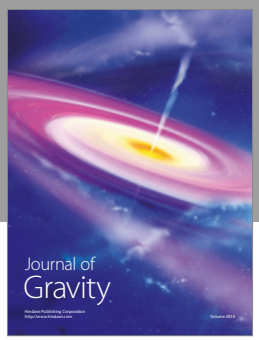

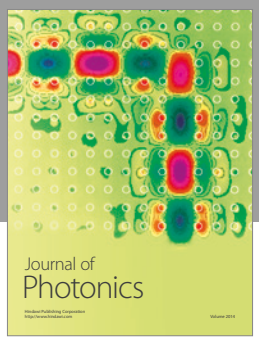

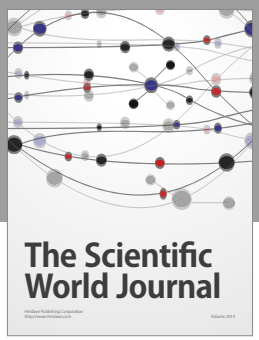

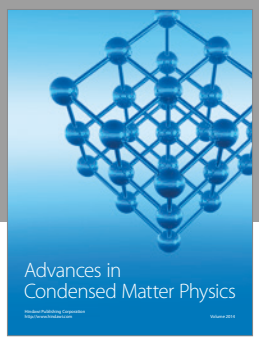

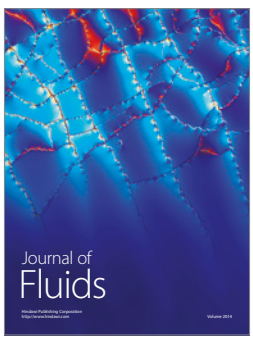

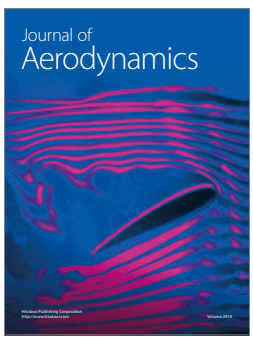

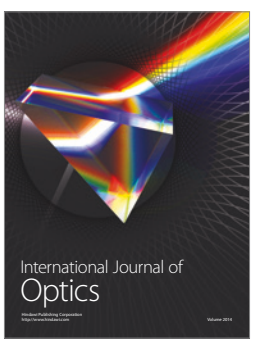

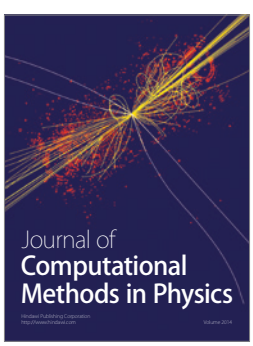

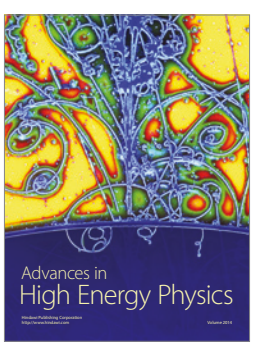

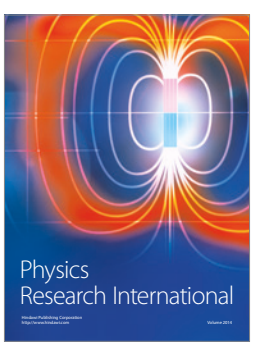

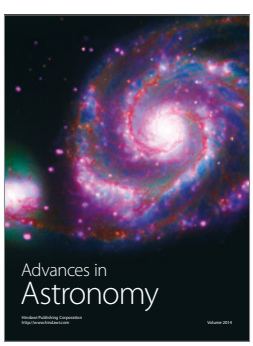

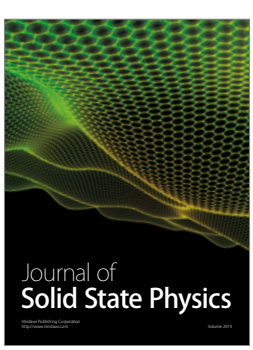

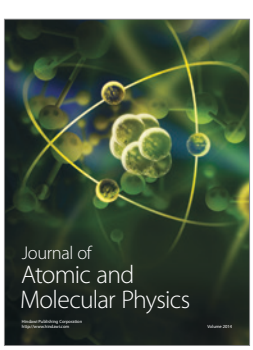

Hindawi

Submit your manuscripts at
https://www.hindawi.com